Widespread nanoflare variability detected with Hinode/XRT in a solar active region

Fabio Reale,[1,2] Sergio Terzo,[1,2] Marco Miceli,[1,2]
James A. Klimchuk,[3]
Ryouhei Kano,[4] Saku Tsuneta[4]

[1]Dipartimento di Fisica, Sezione di Astronomia,
Università di Palermo, Piazza del Parlamento 1, 90134 Palermo, Italy
[2]INAF/Osservatorio Astronomico di Palermo, Piazza del Parlamento 1, 90134 Palermo, Italy
[3]NASA Goddard Space Flight Center, Greenbelt, MD 20771, USA
[4]National Astronomical Observatory, Mitaka, Tokyo 181-8588, Japan
*Fabio Reale; E-mail: reale@astropa.unipa.it

It is generally agreed that small impulsive energy bursts called nanoflares are responsible for at least some of the Sun's hot corona, but whether they are the explanation for most of the multi-million degree plasma has been a matter of ongoing debate. We here present evidence that nanoflares are widespread in an active region observed by the X-Ray Telescope on-board the Hinode mission. The distributions of intensity fluctuations have small but important asymmetries, whether taken from individual pixels, multi-pixel subregions, or the entire active region. Negative fluctuations (corresponding to reduced intensity) are greater in number but weaker in amplitude, so that the median fluctuation is negative compared to a mean of zero. Using MonteCarlo simulations, we show that only part of this asymmetry can be explained by Poisson photon statistics. The re-

mainder is explainable with a tendency for exponentially decreasing intensity, such as would be expected from a cooling plasma produced, e.g., from a nanoflare. We suggest that nanoflares are a universal heating process within active regions.

How the outer atmosphere of the Sun, the solar corona, is heated to several million degrees Kelvin is one of the most compelling questions in space science (*1*). Simple thermal conduction from below is clearly not the answer, since the corona is more than two orders of magnitude hotter than the solar surface. Indeed, whatever mechanism heats the corona must do so in the face of strong energy *losses* from both downward thermal conduction and radiation.

Soft X-ray and EUV images of the corona reveal many beautiful loop structures—arched magnetic flux tubes filled with plasma. The most distinctive of these loops are classified as warm because their temperature is *only* about 1 MK. It is generally agreed that they are bundles of unresolved thin strands that are heated by small energy bursts called nanoflares. Identifiable warm loops account for only a small fraction of the coronal plasma, however. Most emission has a diffuse appearance, and the question remains as to how this dominant component is heated, especially in the hotter central parts of active regions. Is it also energized by nanoflares, or is the heating more steady? Recent observations have revealed that small amounts of extremely hot plasma is widespread in active regions (*2*) and is consistent with the predictions of theoretical nanoflare models (*3*). This suggests that nanoflare heating may indeed be universal. However, the conclusion is far from certain (*4*). The work reported here sheds new light on this fundamental question.

A magnetic strand that is heated by a nanoflare evolves in a well defined manner. Its light curve (intensity vs. time) has a characteristic shape, as shown in Figure 1 (see

on-line material for details). The intensity rises quickly as the nanoflare occurs, levels off temporarily, then enters a longer period of exponential decay as the plasma cools. This particular example comes from a numerical simulation and represents an observation that would be made by the X-Ray Telescope (XRT) on the Hinode spacecraft (*5*). If we could isolate individual strands in real observations, it would be easy to establish whether the heating is impulsive or steady. Unfortunately, this is not the case. The corona is optically thin, so each line of sight represents an integration through a large number overlapping translucent strands. Nonetheless, it may be possible to infer the presence of nanoflares.

Actual light curves exhibit both long and short-term temporal variations. Some of the short-term fluctuation is due to photon statistical noise, but some may be caused by nanoflares. The amplitude of the fluctuations seems to be larger than expected from noise alone (*11–13*). However, this is difficult to determine with confidence, because the precise level of noise depends on the temperature of the plasma, and this is known only approximately in these studies. As we report here for the first time, there is another method for detecting nanoflares from intensity fluctuations that does not depend sensitively on the noise. The light curve in Figure 1 is very asymmetric. The strand is bright for less time than it is faint, and when it is bright it is much brighter than the temporal average. This results in a distribution of intensities that is also very asymmetric. A good measure of the asymmetry is the difference between the median and mean values. The median intensity over the whole simulation (7.0 DN/s) is much less than the mean (16.6 DN/s). This is a generic property of light curves that are dominated by an exponential decay, as is the case with nanoflares. We use this property to demonstrate that nanoflares are occurring throughout a particular active region that we studied in detail. Since the light curve at each pixel in the image set is a composite of many light curves from along the line-of-sight, the asymmetries of the intensity distributions and the differences between

the median and mean values are small. We use both statistical analysis and quantitative modeling to show that the differences are nonetheless significant and consistent with widespread nanoflaring in the active region.

The grazing-incidence X-Ray Telescope (XRT) (*6–8*) detects plasmas in the temperature range $6.1 < \log\ T < 7.5$ with 1 arcsec spatial resolution. Active region AR 10923 was observed on 14 November 2006 near the center of the solar disk. We have studied it previously in other ways (*2, 9*). The observations used for this study were made in the Al_poly filterband starting at 11 UT and lasting $\sim$ 26 min. A total of 303 images were taken with a 0.26 s exposure at an average cadence interval of between 3 and 9 s. No major flare activity or significant change in the morphology occurred during this time. We concentrated on a 256×256 arcsec^2 field of view and used the standard XRT software to calibrate the data. This includes corrections for the read-out signal, flat-field, and CCD bias, as well as dark image subtraction. The images were co-aligned using the jitter information provided with the data.

Figure 2 shows a representative image that has been modified as follows. Because we are interested in low level variations that could be indicative of nanoflares, we ignore pixels with large intensity excursions due to cosmic ray hits, microflares, or other transient brightenings (*11*). We also ignore pixels with longer timescale variability that could result from structures slowly drifting back and forth across the line-of-sight (timescales longer then the tens to hundreds of seconds e-folding time of nanoflare-heated strands). Finally, we ignore pixels where the average count rate is below 30 DN/s, since the signal-to-noise is too small to be useful. A total of 44% of the pixels are rejected on the basis of these criteria. They are displayed as red in the Figure 2. Details are provided in the on-line material.

The light curves of the remaining (green) pixels can be fit satisfactorily well with

a linear regression. The slopes tend to be very small, and there is no preference for increasing or decreasing intensity. Figure 3 shows light curves for two sample pixels with the linear fit in blue; 9-point ($\sim$ 1 min) running averages are shown in green, and the three red exponentials well fit the respective data segments and are overlaid to indicate the evidence for cooling. We measure intensity fluctuations relative to the linear fit according to:

$$dI(x,y,t) = \frac{I(x,y,t) - I_0(x,y,t)}{\sigma_P(x,y,t)} \tag{1}$$

where $I(x,y,t)$ is the count rate (DN/s) at position $[x,y]$ and time t, $I_0(x,y,t)$ is the value of the linear fit at the same position and time, and $\sigma_P(x,y,t)$ is the photon noise estimated from the standard deviation of the pixel light curve with respect to the linear fit. The distribution of the intensity fluctuations is not symmetric at either pixel (see on-line material). There is a slight excess of negative fluctuations (fainter than average emission) compared to positive. The mean fluctuation is 0, by definition, but the median fluctuation (normalized to σ_P) is -0.08 ± 0.07 in the brighter pixel and -0.12 ± 0.07 in the fainter pixel. The uncertainties in the median values have been rigorously computed according to (*10*).

To increase the statistical significance of the measurements, we build larger distributions by adding the individual distributions in subregions of 32×32 pixels. Figure 4 (top-left) shows results for the three sub-regions marked in Figure 2 and for the whole active region. Subtle asymmetries can be detected by eye when compared to the Gaussian distribution shown as a dashed curve for comparison. The top-right panel in Figure 4 shows the distributions of the median values themselves, computed individually at each pixel. There is a clear preference for the medians to be negative. The median of total distributions are between -0.025 ± 0.002 and -0.030 ± 0.002 for the sub-regions and

-0.0258 ± 0.0004 for the active region as a whole. Uncertainties are estimated according to (*10*). The fact that the result is similar for the whole active region is important because it shows that the effect is widespread and real. Were it due simply to random fluctuations, the magnitude would decrease as more and more pixels are included in the statistics.

Photon counting obeys Poisson statistics, and since the Poisson distribution is asymmetric, part of the negative offset of the median values is due to photon noise. We determine how much by performing MonteCarlo simulations to generate synthetic light curves for an appropriate number of pixels. We begin with a constant intensity equal to the mean observed count rate in the pixel, and we add random noise using a Poisson distribution having a standard deviation equal to that of the observed fluctuations relative to the linear fit. Since some of the fluctuation is real, this procedure overestimates the effect of noise. In this way we determine that most 60% of the observed asymmetry is due to photon statistics. The significance of the remainder is at the 5σ level for the subregions and 25σ level for the active region!

We also perform simulations meant to represent cooling plasma by randomly adding pieces of exponential decays onto the constant background intensity (see on-line material for details). Photon noise is included as explained above. The resulting light curves look similar to those in Figure 3. The distributions of the intensity fluctuations agree well with observations, with median values that have a similar negative offset. As an aside, the parameters of the simulations lead to consistent constraints about the loop substructuring and about the energy involved in the heat pulses (see on-line material). We remark that our analysis is entirely independent of filter calibration and highly model-independent.

Previous attempts to determine the nature of coronal heating outside of isolated warm loops have been inconclusive. Our study provides strong evidence for widespread cooling plasma in active region AR 10923. This suggests heating that is impulsive rather than

steady, which in turn suggests that nanoflares play a universal role in active regions. We favor nanoflares occurring within the corona, but our observations may also be consistent with the impulsive injection of hot plasma from below, as has recently been suggested (*14*).

References and Notes

1. J. A. Klimchuk, On Solving the Coronal Heating Problem, *Solar Physics*, **234**, 41 (2006)

2. Reale, F., Testa, P., Klimchuk, J. A., & Parenti, S. , Evidence of Widespread Hot Plasma in a Nonflaring Coronal Active Region from Hinode/X-Ray Telescope, *The Astrophysical Journal*, **698**, 756 (2009)

3. Klimchuk, J. A., Patsourakos, S., & Cargill, P. J. , Highly Efficient Modeling of Dynamic Coronal Loops, *The Astrophysical Journal*, **682**, 1351, (2008)

4. Brooks, D. H., & Warren, H. P. Flows and Motions in Moss in the Core of a Flaring Active Region: Evidence for Steady Heating, *The Astrophysical Journal Letters*, **703**, L10, (2009)

5. Kosugi, T., et al. The Hinode (Solar-B) Mission: An Overview, *Solar Physics*, **243**, 3, (2007)

6. L. Golub, *et al.*, The X-Ray Telescope (XRT) for the Hinode Mission,*Solar Physics*, **243**, 63 (2007)

7. Kano, R., et al. , The Hinode X-Ray Telescope (XRT): Camera Design, Performance and Operations,*Solar Physics*, **249**, 263 , (2008)

8. Narukage, N., et al. , Coronal-Temperature-Diagnostic Capability of the Hinode/X-Ray Telescope Based on Self-Consistent Calibration,*Solar Physics*, 1, (2011)

9. Reale, F., et al. , Science, Fine Thermal Structure of a Coronal Active Region,**318**, 1582 (2007)

10. Hong, J., Schlegel, E. M.,& Grindlay, J. E., New Spectral Classification Technique for X-Ray Sources: Quantile Analysis, *The Astrophysical Journal*, **614**, 508 (2004)

11. Sakamoto, Y., Tsuneta, S., & Vekstein, G. , Observational Appearance of Nanoflares with SXT and TRACE, *The Astrophysical Journal*, **689**, 1421 (2008)

12. Sakamoto, Y., Tsuneta, S., & Vekstein, G. , A Nanoflare Heating Model and Comparison with Observations, *The Astrophysical Journal*, **703**, 2118 (2009)

13. Vekstein, G. , Probing nanoflares with observed fluctuations of the coronal EUV emission, *Astronomy & Astrophysics*, **499**, L5 (2009)

14. De Pontieu, B., et al. , The Origins of Hot Plasma in the Solar Corona, *Science*, **331**, 55, (2011)

15. Hinode is a Japanese mission developed and launched by ISAS/JAXA, collaborating with NAOJ as a domestic partner, NASA and STFC (UK) as international partners. Scientific operation of the Hinode mission is conducted by the Hinode science team organized at ISAS/JAXA. This team mainly consists of scientists from institutes in the partner countries. Support for the post-launch operation is provided by JAXA and NAOJ (Japan), STFC (U.K.), NASA, ESA, and NSC (Norway). F.R., S.Te. and M.M. acknowledge support from Italian Ministero dell'Università e Ricerca and Agenzia Spaziale Italiana (ASI), contracts I/015/07/0 and I/023/09/0. The work of J.A.K. was supported by the NASA

Supporting Research and Technology and LWS Targeted Research and Technology programs. We thank M. Caramazza and Y. Sakamoto for help in data analysis. F.R. provided the scientific leadership, led the data analysis and modeling, and wrote the manuscript. S.Te. performed the data analysis. M.M. performed the MonteCarlo simulations. J.A.K. helped in the data analysis and modeling, and wrote the manuscript. S.Ts. and R.K. selected the data and provided support to scientific leadership and to the data analysis.

Fig.1: Light curve in the XRT Al_poly filterband obtained from a hydrodynamic simulation of the plasma confined in a loop strand ignited by a heat pulse (nanoflare). The heat pulse lasts 60 s and brings the strand to a maximum temperature $\log T \approx 7$.

Fig.2: Active region AR 10923 observed with the Hinode/XRT Al_poly filter on 14 November 2006 at 11 UT. We distinguish between pixels accepted (green) and rejected (red) for the analysis. The color scales are powers of the intensity (0.5 and 0.1 for green and red respectively), with maxima of 57 DN/s and 1171 DN/s respectively. We mark three subregions (frames) which are analyzed specifically. We show in Figure 3 the light curves of two pixels (indicated by the arrows).

Fig.3: Light curves of two selected pixels indicated in Figure 2. The linear fits are marked (blue lines); 9-point ($\sim$ 1 min) running averages are shown (green). Exponentials lines (red) well fit the respective data segments.

Fig.4: Statistical analysis of the fluctuations of the pixel light curves with respect to the linear fit in three selected regions (marked with the same colors as in Figure 2) and in the whole active region (black histogram). We show the distributions of the fluctuations normalized to the nominal Poisson noise and the distributions of the medians normalized to their standard deviation. A Gaussian centered on zero and unit width is plotted for reference (dashed line).

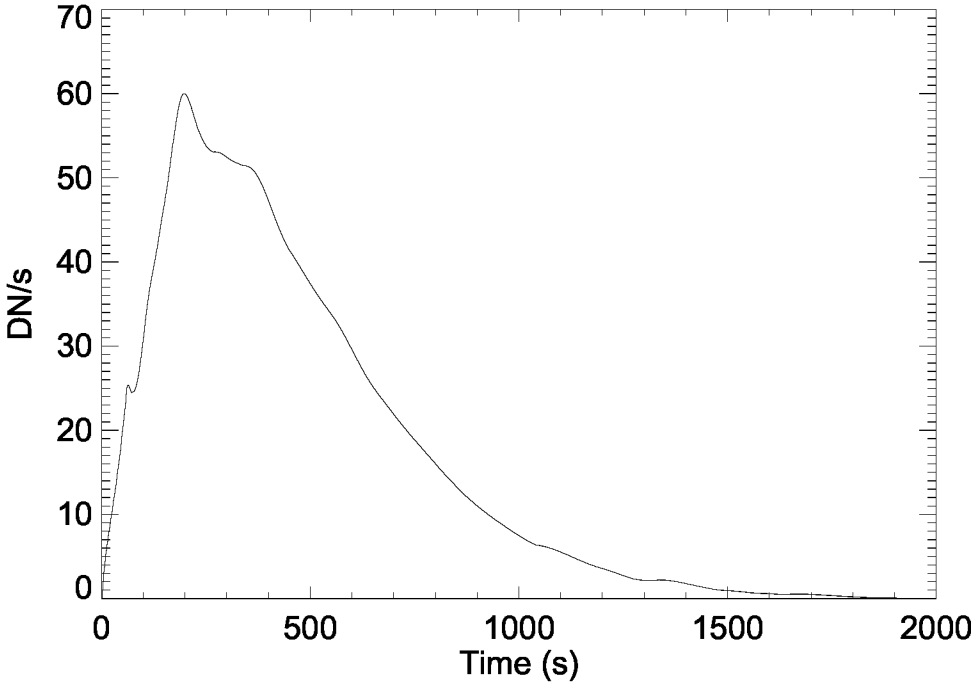

Figure 1:

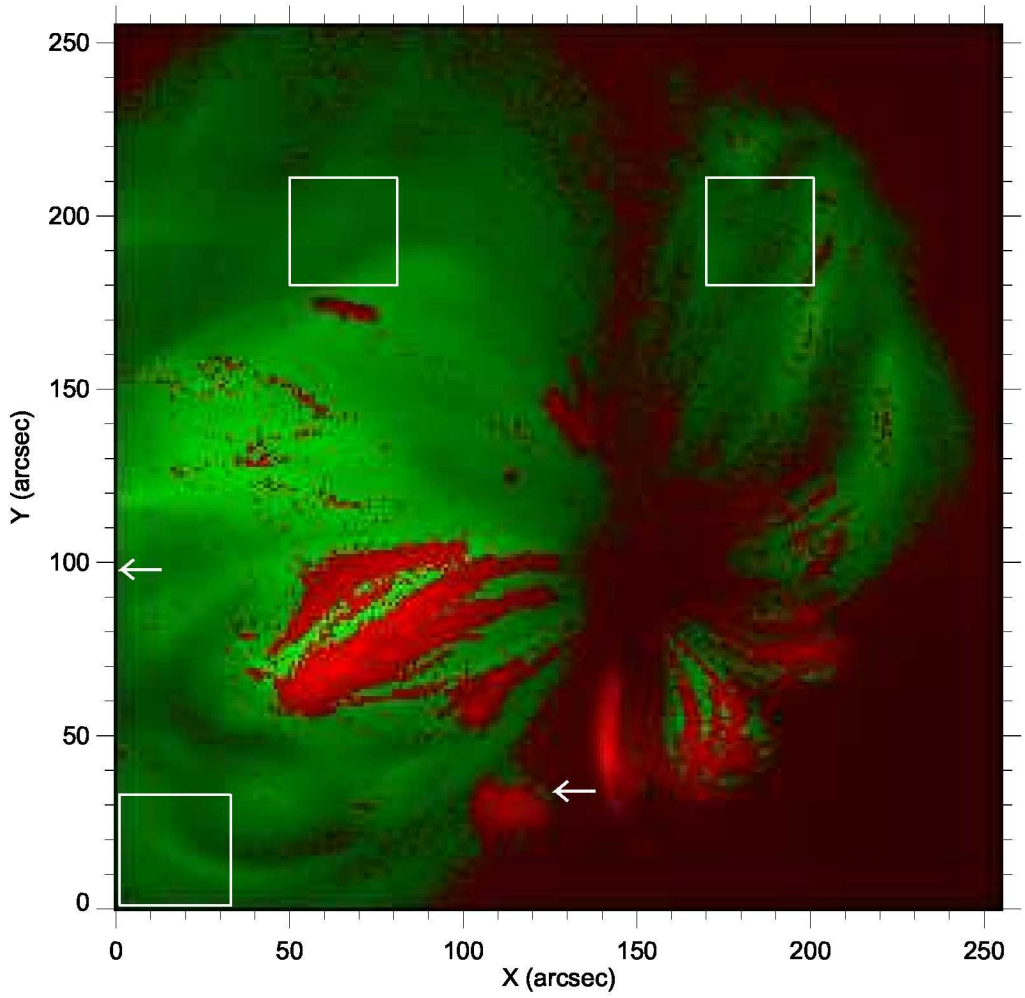

Figure 2:

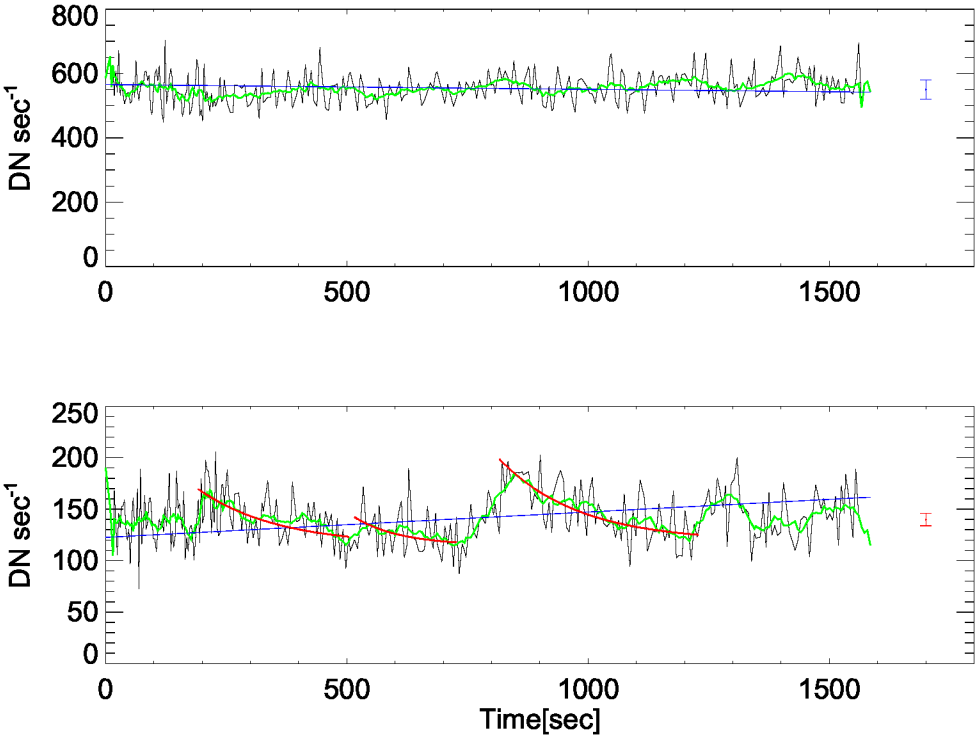

Figure 3:

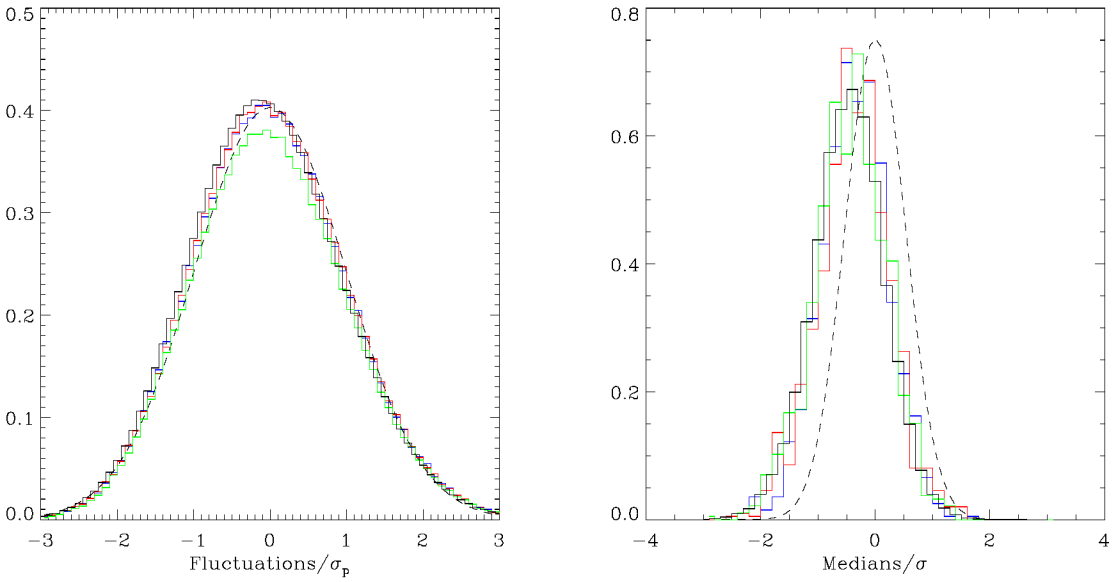

Figure 4: